Interplay between dynamic screened f-f interaction and $\mathbf{s_k}\cdot\mathbf{s}_f$ interaction in Ce systems

F. López-Aguilar, J. Costa-Quintana, and M. M. Sánchez-López
Grup d'Electromagnetisme, Departament de Física, Edifici Cn, Universitat Autònoma de Barcelona, E-08193 Bellaterra, Barcelona, Spain
(Received 19 March 1997)

Two complementary analyses for the electronic structure of Ce systems are given. The first is performed from the renormalized density of states (DOS) deduced from the interacting Green's functions. These Green's functions are obtained from a self-energy calculated from a multiband Hubbard Hamiltonian and using the random phase approximation to account for the dynamical f-f screened interactions. The resulting DOS presents agreements and discrepancies with the spectral data yielded by direct and inverse photoemission. The theoretical and experimental f widths next to the Fermi level imply f-electron masses that are in strong contradiction with those obtained from the heavy-fermion specific heat. We have carried out a second analysis that complements the first one, since it considers the spin-exchange between extended states and a spin-field that is completely excluded from the first calculation. By the marriage of the results obtained in the first calculation with those of the second analysis, we can relate the photoemission spectra and de Haas–van Alphen masses with the measurements of the contribution of the low-energy quasiparticles to the specific heat and the magnetic susceptibility. [S0163-1829(97)08328-8]

I. INTRODUCTION

The phenomenology of strongly correlated systems can be explained by considering the interplay between the dynamical screening of the f-f interactions that arises from the charge fluctuations and the magnetic interactions governed by the spin fluctuations plus spin correlations, which can be analyzed from the Kondo lattice model (KLM).[1–3] An interesting fact originated by this interplay is that there are experimental results that seem to be in better agreement with the charge-fluctuation phenomenology whereas other experiments seem to give support to the magnetic behaviors.[3] While the direct and inverse photoemission spectroscopy can be partially justified from the dynamic screening coming from the f-charge fluctuations,[2–4] the specific heat (C_V) of these materials implies electronic masses two or three orders of magnitude larger than those expected from the spectroscopy measurements.[3,5] This seems to suggest that the magnetic behavior plays an important role in the arising of the large electronic mass of the heavy-fermion (HF) state. On the other hand, the de Haas–van Alphen (dHvA) oscillation of the susceptibility implies similar electronic masses to those deduced from photoemission.[3] The strong variation of C_V with temperature T leads to excluding the renormalization self-energy effects as the cause for this mass enhancement,[3,5] since these effects become practically insensitive to the T variation. On the contrary, it seems to be related to either a change in entropy that takes place above a characteristic temperature when a decrease of magnetic order is produced by the loss of magnetic correlations or the existence of collective states, or even the addition of the two effects.[3]

The Ce systems have an electron located in the f band[1,5,6] and this condition allows one to consider some of these compounds as paradigmatic examples of strongly correlated systems in which the contradictory interplay between charge and spin fluctuations is remarked upon. This is so because the f electrons may form a quasiparticle band[7–9] that crosses the Fermi level (E_F), and thus the charge and spin fluctuations in the f-electron atoms can be large. These materials present, within ± 3 eV around E_F, an almost universal electronic structure, dominated by two energy scales, which displays three characteristic structures.[5,6,10,11] The first one is located at $\simeq -2.5$ eV below the Fermi level and it is experimentally detected by direct photoemission.[5,6] Its origin is unambiguously assigned to the $4f^0$ final state of the photoelectron emission (i.e., $4f^1$ initial state), and the corresponding peak in the density of states (DOS) can be assimilated to the lower Hubbard band (LHB). The second structure, located at $\simeq 4$ eV above E_F, corresponds to the $4f^2$ final state. It is detected by the inverse photoemission process[10,11] and it can be identified with the upper Hubbard band (UHB). This band is physically interpreted as the $E(\mathbf{k})$ dispersion of the $4f^2$ configuration that propagates through the crystal with quasimomentum $\mathbf{k}$. Finally, the most intriguing $4f$ resonance is located in the energy region near E_F (Refs. 5, 6, 10–13, and 21) and is split in several features. This middle-energy structure is generally constituted by two peaks below E_F (Refs. 5, 6, 10 and 11) that are detected, therefore, by direct photoemission (at $\simeq -300$ and $\simeq -30$ meV) and another peak located just above E_F that is displayed in the bremsstralung spectroscopy. This triple structure is out of the simple LHB/UHB scheme and its origin has presented strong controversy. Since it is located between the LHB and UHB, it corresponds to $4f$ resonances that can be called middle-energy Hubbard bands (MHB). These resonances may be linked to an intermediate n_f occupation arising from the charge fluctuations due to the transferences of $4f$ electrons between Ce atoms. The existence of this intermediate state can be justified by the band character of the $4f$ states and therefore it would be related to the indetermination of the n_f occupation per $4f$ atom in the band model.[7–9] In any case, the middle-energy structure is consistent with a transference of spectral weight between the upper and lower Hubbard

bands.[12] Obviously, this interpretation enters in competition with the idea that these near-E_F peaks are related with the Kondo effect resonance described by the impurity Anderson model[6] (IAM). The IAM can provide a good description in the cases of completely localized $4f$ states and conduction electrons interacting via hybridization with the magnetic impurities (that do not interact themselves). It is an important model for performing a heuristic analysis that describes generally the strongly correlated systems, but the realistic cases that present $4f$ band states should be treated via the lattice Anderson Hamiltonian, whose solution is not so simple as that of the IAM.

However, a detailed analysis of the low-energy properties that arise from the thermodynamical, spectroscopic, and dHvA measurements induce one to think that the consideration of only charge fluctuation effects arising from the dynamical screening are unable to reconcile the experimental data. We believe that even a good understanding of the MHB requires the combination of the f-charge and spin fluctuation effects. But above all, we wish to emphasize that the effects of both fluctuations should be complementarily taken into account to conciliate the direct and inverse photoemission data and the dHvA determination of the Fermi surface with the thermodynamical masses of the low-energy quasiparticles and the magnetic susceptibility characteristic of the HF state of some Ce systems.

From a theoretical point of view, Anderson[14] suggested some years ago that for large values of the energy U in the Hubbard or Anderson-lattice Hamiltonian, the dynamics of the f-charge fluctuations and the spin exchange are essentially independent. Thus, for experimental and theoretical reasons, our strategy will consist in studying both contributions separately. Therefore, we analyze in this paper the electronic structure of a characteristic HF compound within two complementary models in order to discriminate the different sources of the two antagonistic properties: on the one hand, the spectroscopic features (basically justified via dynamical screening, although the KLM analysis is needed for completeness), and on the other hand, the enhancement of the electronic mass and the magnetic susceptibility (whose origin is closer to the magnetic properties coming from the KLM). The superposition of the results obtained from the two models allows us to find certain theoretical coherence between them and agreement with the experimental results.

II. CHARGE FLUCTUATION EFFECTS

In this section we calculate the one-body electronic structure of the characteristic HF compound $CeSi_2$. We have chosen this material because there is extensive literature[5,6,11] about its photoemission spectroscopy and a strong controversy in the interpretation of these results, which is centered exactly in the title of this work (i.e., in the interplay between the charged screening and magnetic exchange). Therefore, this compound is a perfect challenge for testing our double analysis. The electronic structure of $CeSi_2$ is calculated using a method appropriate for determining the one-body spectrum of any transition-metal, rare-earth, and actinide-based compound, as well as others that constitute the group of strongly correlated electronic systems (SCS). This method is valid for any approximation to the self-energy, and it can also deal with different crystal potentials for each spin-orbital symmetry, thus allowing one to reproduce both the Hund's rule and the Hubbard splitting. The self-energy approach considered for $CeSi_2$ is obtained from the multiband Hubbard Hamiltonian and takes into account the extended random phase approximation to the effective interaction. The calculation of the electronic structure is performed by diagonalizing the inverse of the Green's function[15] ($\tilde{\mathbf{G}}$), which can be expressed as:

$$\tilde{\mathbf{G}}=\tilde{\mathbf{G}}^0+\tilde{\mathbf{G}}^0\ \ \tilde{\mathbf{M}}\tilde{\mathbf{G}}, \tag{1}$$

where the matrix $\tilde{\mathbf{M}}$ stands for the self-energy and $\tilde{\mathbf{G}}^0$ is the noninteracting system's Green function. The $\alpha\beta$ matrix element of $\tilde{\mathbf{G}}$ is given by

$$G^{-1}_{\alpha\beta}(\mathbf{k},\omega)=(\omega-\varepsilon^0_{\mathbf{k}\alpha}\pm i\theta^+)\,\delta_{\alpha\beta}-M_{\alpha\beta}(\mathbf{k},\omega), \tag{2}$$

where $M_{\alpha\beta}(\mathbf{k},\omega)$ is the matrix element of the self-energy calculated between two eigenstates $|\mathbf{k}\alpha\rangle$ and $|\mathbf{k}\beta\rangle$ of the noninteracting system's Hamiltonian (H_{LDA}) of eigenvalues $\varepsilon^0_{\mathbf{k}\alpha}$ and $\varepsilon^0_{\mathbf{k}\beta}$, respectively ($\alpha$ and β are band indexes). The interacting Hamiltonian of the SCS has nonzero terms only between electrons located in strongly correlated orbitals belonging to f atoms. Therefore, the self-energy affects only the strongly correlated component of the band states.[4] The matrix of Eq. (2) can then be written as

$$G^{-1}_{\alpha\beta}(\mathbf{k},\omega)=(\omega-\varepsilon^0_{\mathbf{k}\alpha}\pm i\theta^+)\,\delta_{\alpha\beta} - \sum_{mm'}\sum_{\nu\nu'}\langle\mathbf{k}\alpha|m\nu\rangle M^{\nu\nu'}_{mm'}(\omega)\langle m'\nu'|\mathbf{k}\beta\rangle, \tag{3}$$

where $\langle\mathbf{k}\alpha|m\nu\rangle$ is the projection of a certain H_{LDA} eigenstate $|\mathbf{k}\alpha\rangle$ on a strongly correlated component m centered in the ν atom of the primitive cell. We have performed a LDA band-structure calculation within a standard symmetrized augmented plane wave method and we have determined $\varepsilon^0_{\mathbf{k}\alpha}$ and $\langle m\nu|\mathbf{k}\alpha\rangle$, whose expression is

$$\langle m\nu|\mathbf{k}\alpha\rangle=\frac{i4\pi g}{n_p}\sum_i\sum_R v(\mathbf{k}_i,\varepsilon^0_{\mathbf{k}\alpha})[\Gamma^{\alpha}_{11}(R)]^* \times\exp(iR\mathbf{k}_i\cdot\mathbf{r}_\nu)\frac{j_l(R\mathbf{k}_i,S_\nu)}{u_l(S_\nu,\varepsilon^0_{\mathbf{k}\alpha})}\ \mathcal{Y}_p(\theta_i,\varphi_i) \times\sqrt{\int r^2\,dr|u_l(|\mathbf{r}-\mathbf{r}_\nu|;\varepsilon^0_{\mathbf{k}\alpha})|^2}. \tag{4}$$

The former equation follows the standard notation.[4] The coefficients $v(\mathbf{k}_i,\varepsilon^0_{\mathbf{k}\alpha})$ define the $|\mathbf{k}\alpha\rangle$ state and are obtained in this first LDA calculation.

The matrix of Eq. (3) must be constructed and diagonalized for each point $\mathbf{k}$ of the irreducible Brillouin zone. The self-energy $M^{\nu\nu'}_{mm'}(\omega)$ usually depends on the frequency because it accounts for the dynamical screening between the states, thus it affects differently states of different energies. Therefore, the matrix that must be diagonalized is a function of ω and obviously of $\mathbf{k}$, and its eigenvalues are also a function of ω and $\mathbf{k}$. According to the usual notation in band

theory, we write these eigenvalues as $E_{\mathbf{k}\alpha}(\omega)$, where the subindex $\mathbf{k}\alpha$ indicates now an eigenstate of the interacting system instead of a H_{LDA} eigenstate. Looking at Eq. (3), it is straightforward that $\tilde{\mathbf{G}}$ is a complex non-Hermitian matrix for any complex self-energy and its diagonalization will give complex eigenvalues of the form

$$E_{\mathbf{k}\alpha}(\omega)=\varepsilon_{\mathbf{k}\alpha}(\omega)+i\,\gamma_{\mathbf{k}\alpha}(\omega). \tag{5}$$

Then, $\tilde{\mathbf{G}}$ can be written in the diagonalized form

$$G_{\mathbf{k}\alpha}(\omega)=[\,\omega-\varepsilon_{\mathbf{k}\alpha}(\omega)-i\,\gamma_{\mathbf{k}\alpha}(\omega)\,]^{-1}. \tag{6}$$

The spectrum of the interacting system is given by the poles (ω_0) of the Green function. Thus, the intersections of the straight line $y=\omega$ with the function $y=E_{\mathbf{k}\alpha}(\omega)$ must be calculated. The real part of the pole $[\,\varepsilon_{\mathbf{k}\alpha}(\omega_0)]$ is the spectrum of the quasiparticle state $|\mathbf{k}\alpha\rangle$ while its imaginary part $[\,\gamma_{\mathbf{k}\alpha}(\omega_0)]$ is inversely proportional to the quasiparticle lifetime.

The renormalized DOS is calculated from the spectral functions $A_{\mathbf{k}\alpha}(\omega)=-(1/\pi)\mathrm{Im}G^R_{\mathbf{k}\alpha}(\omega)$. Developing the function $\omega-\varepsilon_{\mathbf{k}\alpha}(\omega)$ of Eq. (6) in a Taylor series around the solution $\omega_0=\varepsilon_{\mathbf{k}\alpha}(\omega_0)$, the spectral function takes the form:

$$A_{\mathbf{k}\alpha}(\omega)=\frac{1}{\pi}\,\frac{Z^2_{\mathbf{k}\alpha}(\omega_0)|\,\gamma_{\mathbf{k}\alpha}(\omega_0)|}{[\,\omega-\varepsilon_{\mathbf{k}\alpha}(\omega_0)]^2+[Z_{\mathbf{k}\alpha}(\omega_0)\,\gamma_{\mathbf{k}\alpha}(\omega_0)]^2}, \tag{7}$$

where the renormalization factor $Z_{\mathbf{k}\alpha}(\omega_0)$ that corresponds to the quasiparticle state of energy $\varepsilon_{\mathbf{k}\alpha}(\omega_0)$ is given by

$$Z^{-1}_{\mathbf{k}\alpha}(\omega_0)=1-\left.\frac{\partial\varepsilon_{\mathbf{k}}\alpha}{\partial\omega}\right|_{\omega=\omega_0}. \tag{8}$$

A. Self-energy used in the calculation

We consider a self-energy operator that takes into account the dynamical screening of the f-f interactions produced by the charge fluctuations. The simplest perturbative series that yields the basic features of the electronic structure of the strongly correlated systems is the random phase approximation[16,4] (RPA) obtained from the multiband Hubbard Hamiltonian. Then, we will calculate the electronic structure considering only the dynamic screening of the f-f interaction and excluding the Kondo effect. The purpose of including in this first part of the work the charge fluctuation effects in the self-energy while excluding the spin fluctuations is to discern the role of the charge dynamic screening in the MHB $4f$ resonance independently of other causes that could also influence its appearance. Starting from a multiband Hubbard Hamiltonian and going beyond mean-field theory, we calculate the self-energy operator in the RPA. Only the exchange diagram for the self-energy (the so-called ''open oyster'' diagram) is considered and the noninteracting DOS of every SC m orbital is modeled by a double Lorentzian curve.[4] The self-energy that affects each m orbital then has the following expression:

$$M^{\nu\nu'}_{mm'}(\omega)=\delta_{mm'}\delta_{\nu\nu'}U^{\nu}_m(\tfrac{1}{2}-n^{\nu}_m)+\delta_{mm'}\delta_{\nu\nu'}U^{\nu}_m\,\frac{\Omega^2_{m\nu}-Y^2_{m\nu}}{2\Omega_{m\nu}}\times\left(\int_{-\infty}^{E_F}\frac{N^{\nu}_m(x)dx}{\omega+\Omega_{m\nu}-x-i\,\theta^+}+\int_{E_F}^{\infty}\frac{N^{\nu}_m(x)dx}{\omega-\Omega_{m\nu}-x+i\,\theta^+}\right). \tag{9}$$

$\Omega_{m\nu}$ and $Y_{m\nu}$ depend on the band parameters that describe the noninteracting DOS, as well as on the occupation n^{ν}_m and on-site Coulomb correlation U^{ν}_m of the m orbital of the ν atom, through the equations (see Ref. 4)

$$\Omega^2_{m\nu}=(\gamma^{\nu}_m-i\Gamma^{\nu}_m)^2+4U^{\nu}_m n^{\nu}_m(1-n^{\nu}_m)(\gamma^{\nu}_m-i\Gamma^{\nu}_m), \tag{10}$$

$$Y^2_{m\nu}=(\gamma^{\nu}_m-i\Gamma^{\nu}_m)^2, \tag{11}$$

where γ^{ν}_m is the separation between peaks in the input DOS and Γ^{ν}_m is the sum of their half-widths. The parameter n^{ν}_m concerns the average occupation number of spin bands whose maximun value is 1, therefore a nonmagnetic ordered material with a $4f^1$ configuration can have two $n^{\nu}_m=0.5$. The screening of the on-site correlation yields the ω-dependent terms of the self-energy in Eq. (9) and correct the $U^{\nu}_m(1/2-n^{\nu}_m)$ term that corresponds to the first-order diagram. By inspecting Eqs. (9)–(11) we see that the energy-dependent terms of the self-energy tend to zero when the bandwidths of the noninteracting system increase and/or the m orbital is either completely occupied or unoccupied (since then $\Omega^2_{m\nu}=Y^2_{m\nu}$). When this is not the case, the self-energy of Eq. (9) has two maxima at energies next to $\omega=\pm\Omega_{m\nu}$. Because of this peaked shape of the self-energy, there can be several cuts (at least three) between its real part $\mathrm{Re}M_m(\omega)$ and the straight line $y=\omega-\varepsilon^0_m$ (ε^0_m is an LDA eigenvalue), i.e., there can be several poles of the Green function for each energy of the noninteracting system. Therefore the interacting DOS can show the characteristic multipeak structure of the Ce systems. This behavior of the RPA self-energy is also shown by other approximations that are more sophisticated, such as the one deduced from the three-body Fadeev equations by Calandra and Manghi[17] (see Ref. 18 for a more detailed comparison with other approximations to the self-energy).

B. Results

As stated above, $CeSi_2$ is an ideal material for testing our approach since there exists a large number of direct and inverse photoemission studies on this compound, and a relatively recent strong controversy not solved yet.[5,6,11] $CeSi_2$ is a nonmagnetic material whose susceptibility does not show any magnetic order between 70 and 0.1 K, and whose linear coefficient of the specific heat is $\simeq$100 mJ/K^{2}mole,[5,6,11] implying bandwidths of around 10 meV only possible within the f systems. The core of the controversy lies in the interpretation of the spectroscopic data. Joyce *et al.*[5] maintain that the direct photoemission results cannot be explained through the light of the IAM because the low-energy structure predicted by this model is too narrow when compared to spectroscopic results. On the other hand, the predicted low-

energy peak is at least 10 times wider than what would correspond to the large specific heat of this compound.[5,6] In addition, and according to this group, the temperature evolution is simply due to the phonon broadening and the Fermi function. Besides, they assert that the correlation predicted by the IAM of the location and intensity of the Kondo peak with its width, as well as its temperature dependence, does not agree with the experimental results, since the low-energy pattern of the spectrum below E_F is quantitatively similar for several materials with very different Kondo temperatures.[5] On the contrary, Malterre *et al.*[6,10,11] support the idea that the IAM provides a basic description of the experimental results of the direct and inverse photoemission spectroscopies.[6,10,11] According to their opinion, the low-energy peaks are due to the impurity Kondo effect, and the evolution of the experimental photoemission data with the temperature can be understood within the IAM. The quantitative discrepancies are attributed, by this group, to crystal, spin-orbit, and final-state effects as well as to the insufficient resolution of the experiments.

The spectroscopic MHB of $CeSi_2$ presents the multipeak $4f$ structure[5,6,11] described above. The width of the MHB is around $\simeq 0.4$ eV below and above E_F, i.e., $\simeq 0.8$ eV, which is very large for a standard HF system as $CeSi_2$.[5,6,10,11] In our results of Fig. 1(b) the three peak structures are displayed: the ones located at ~ -3 and ~ 4 eV that correspond, respectively to the $4f^0$ and $4f^2$ final states in the photoemission process, along with the MHB structure. This last structure is shown in detail in Fig. 1(d). It displays three substructures: one of them just below E_F at $\simeq -30$ meV, the second one at $\simeq -110$ meV, and a shoulder just above E_F at $\simeq 30$ meV. The total width is around two orders of magnitude larger than the results expected from the thermodynamical measurement of the specific heat.[5,6,11] On the other hand, we have performed a calculation considering the temperature dependence of the self-energy. These results are not shown in the figure because the differences with those at $T=0$ are negligible since the only source of temperature effects in this type of calculation arises from the Fermi function.

The calculated f-DOS [Figs. 1(a), 1(b), and 1(d)] presents agreements and discrepancies with the experimental data of Ref. 5 and Refs. 6 and 11. The agreements are as follows: (i) the appearance of three structures near E_F. To our knowledge, this is a new theoretical result with respect to those obtained within the mean-field approximation to the Hubbard Hamiltonian, which do not yield any kind of MHB. According to our interpretation, the central features arise from the transference of spectral weight between the LHB and UHB, which is experimentally detected in several strongly correlated materials, both in HF systems[12] and high T_c superconductors,[20] (ii) the width of each feature and their total bandwidths agree with the experimental data, and (iii) the location of the two features just below and above E_F (at $\simeq -30$ and $\simeq 30$ meV) agrees with that obtained in Ref. 5 and Refs. 6 and 11. The discrepancies are as follows: (i) the inner feature is experimentally located at $\simeq -300$ meV while in our results it is at $\simeq -110$ meV. This discrepancy can be explained because we have obtained the energy splitting of the two structures below E_F by means of a quasiparticle band-structure calculation in which the self-energy effects are added to the crystal effects and the hybridization with other extended states, but without considering the spin-orbit correction. This correction is estimated to be around 200 meV, and this is indeed the difference between the experimental data and our results. (ii) The shoulder located at $\simeq 30$ meV in our results is a true peak in the $CeSi_2$ experimental results.[11] However, this peak is softened when measured in $CeSi_{1.6}$,[11] which means that it contains contributions from $3p$ states of Si, and therefore, the tendency is to polish the discrepancy with our results when only the $4f$ contribution is considered (we will justify this $3p$ contribution in the second part of this work, devoted to the Kondo lattice effects). (iii) The first peak below and closer to E_F in Fig. 1(d) is shorter than the inner peak located at -110 meV, while photoemission experimental results show the opposite.

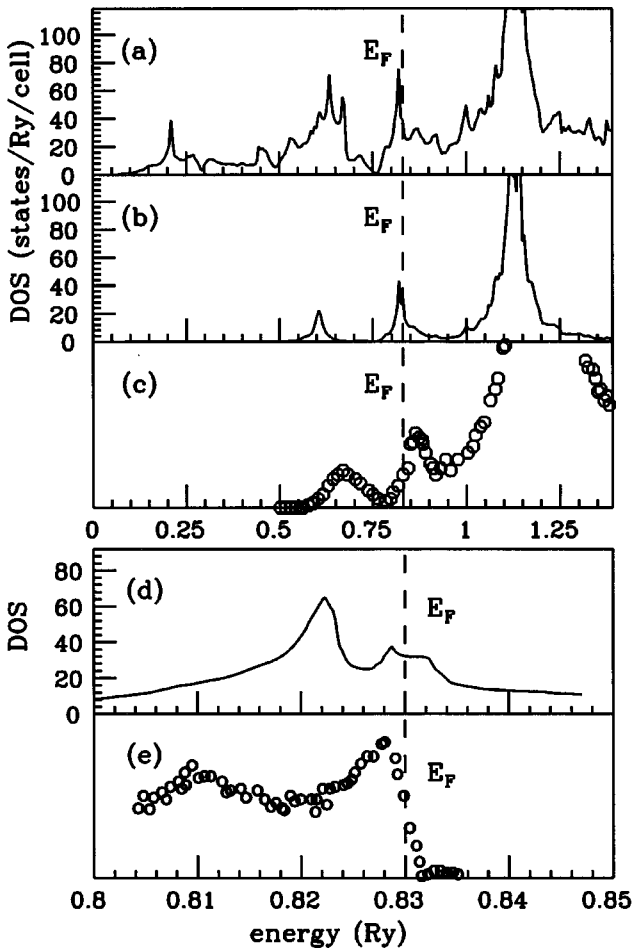

FIG. 1. (a) Total DOS of $CeSi_2$ obtained with a RPA self-energy with $U=0.42$ Ry; (b) corresponding partial f DOS of $CeSi_2$; (c) direct and inverse photoemission spectrum (arbitrary units) of $CeSi_2$ from Ref. 11; (d) detail of the middle Hubbard band of (b) (see main text); (e) near-E_F $CeSi_2$ photoemission spectrum (arbitrary units) from Ref. 6.

From the results of this section, which are summarized in Fig. 1, we conclude that the mass renormalization produced by the combination of the self-energy effects plus the f-p hybridization is unable to give masses of around 100–1000 times the free-electron mass.[3,5] Although the results concern a particular Ce system, the arguments presented in this section hold also for other Ce-based HF materials, since the pattern of their electronic structure is almost universal. It is

very difficult to foresee whether other self-energy approximations, in line with that used in this calculation, will be valid for obtaining the required mass enhancement, since the concomitance of the magnetic properties (such as certain antiferromagnetic couplings) indicate other causes for the HF state. In other cases, as in the U-related compounds UIr_3, UPt_3, and UAu_3 the consideration of a second-order self-energy for obtaining the mass-enhancement factor[21] $[1-(\partial \mathrm{Re}\ \Sigma^{(2)}(\omega)/\partial\omega)]^{-1}$ seems to be sufficient to conciliate the dHvA measurements with the specific heat. However, we notice that these materials present important differences with the Ce HF compounds and in particular with $CeSi_2$, since the U value for these U compounds is around 2 eV,[21] while for the Ce systems it is around 7 eV. Moreover, the delocalization of the $5f$ band states is larger than that of the $4f$ band states. These points are crucial in the appearance of the characteristic structures of both the MHB and the LHB/UHB. In addition, the existence of a controversy between different experimental groups has provided highly refined experimental results in $CeSi_2$, which require one to improve the theoretical explanation for the spectroscopical and other experimental data. Therefore, in the case of Ce alloys, it is necessary to think of other reasons (as the Kondo lattice effects) for conciliating the giant specific heat with the features of the electronic structure.

III. KONDO-LATTICE ANALYSIS

The KLM is generally regarded as a canonical model for Ce-based HF compounds.[1,22–25] The KL model assumes that the high on-site Coulomb repulsion can inhibit the f-charge fluctuations, allowing the spin to fluctuate freely. This analysis considers a system with noninteracting extended band states and an exchange interaction between the spin of these conduction states with a localized spin field arising from the f levels. These levels should be sufficiently deep to prevent the contribution of the corresponding charged particles in the low-energy physics. Therefore, this model is complementary to the band model considered in the former section. The results of the former section fix a ground state ($4f^1$ initial state in the photoemisions process) with an electron in the f level is located at $\simeq$ 2.5 eV and an energy $U\simeq$ 6 eV. Both data imply initial good conditions for considering the KLM analysis since we have a deep $4f^1$ level and an energy U, which in principle forbids the double $4f$ occupation and therefore the spin in each Ce site is $s=1/2$. Despite many years of investigations[22,23] a theoretical explanation of the HF state[1,24,25] based on this model or on the Anderson lattice still remains incomplete and controversial. The clear example of this situation is the present debate on whether the very high values of the low-temperature specific heat and magnetic susceptibility are due to charged[26,27] or neutral[3] heavy fermions.

In this section, we present a treatment of the KLM that leads to results that, coupled with those of the first calculation, can explain in a better way the essential HF phenomenology. The technical and detailed exposition of the mathematical formalism of the KLM analysis is quite extensive and it has been published elsewhere.[28] Here, we will briefly describe the essential ideas underlying this formalism with the aim of showing how it leads to a remarkable physical result, namely, the location of strongly correlated charged modes, their location with respect to E_F, and their influence in the appearance of the HF state.

We consider a KLM consisting of a conduction band that in Ce systems such as $CeSi_2$ can correspond to the non-f electrons (for instance the $3p$ states arising from Si and/or $5d/6s$ from Ce), coupled to a lattice of $s=1/2$ local moments by an exchange interaction, namely,

$$H=\sum_{\mathbf{k},\alpha}\ \varepsilon_{\mathbf{k}}c^{\dagger}_{\mathbf{k}\alpha}c_{\mathbf{k}\alpha}+J\sum_{i}\ \mathbf{S}_{ei}\cdot\mathbf{S}_{fi}\,. \tag{12}$$

$\mathbf{S}_{ei}=1/2\Sigma_{\alpha,\beta}c^{\dagger}_{i\alpha}\boldsymbol{\sigma}_{\alpha\beta}c_{i\beta}$ is the spin of the conduction electrons and $\mathbf{S}_{fi}$ is the ($s=1/2$) local spin at site i corresponding to the localized f states. For simplicity, we consider a constant density of states D and a half-filled conduction band. Energy units are taken to normalize the bandwidth, which implies that $D=1$ and $-1/2\leqslant\varepsilon_{\mathbf{k}}\leqslant 1/2$. The algebra of local spins is described by the following operators: $s_{\pm 1,i}\equiv\sqrt{2}(S^{x}_{fi}\pm iS^{y}_{fi})$ and $s_{0,i}\equiv 2S^{z}_{fi}$. They satisfy the multiplication properties ($s_{0,i}s_{1,i}=s_{1,i}$, $s_{0,i}s_{-1,i}=-s_{-1,i}$, $s_{1,i}s_{-1,i}=1+s_{0,i}$, etc.) in such a way that the product of spin operators is maintained at the same lattice site.

When $J=0$, the two subsystems are noninteracting and the ground state $|\Phi_0\rangle$ consists of a degenerate spin lattice plus a Fermi sea with electrons and holes as elementary charged excitations. If $\mathbf{q}$ ($\mathbf{p}$) denotes a wave vector located below (above) the Fermi surface ($\varepsilon_{\mathbf{q}}<0$, $\varepsilon_{\mathbf{p}}>0$), the annihilation operators corresponding to electrons and holes are given by $e_{\mathbf{p}\alpha}=c_{\mathbf{p}\alpha}$ and $h_{\mathbf{q}\alpha}=c^{\dagger}_{-\mathbf{q},-\alpha}$, respectively. The expression of the Hamiltonian (12) in terms of the operators $e_{\mathbf{p}\alpha}$, $h_{\mathbf{q}\alpha}$, and $s_{l,\mathbf{k}}$ ($s_{l,\mathbf{k}}=N^{-1/2}\Sigma_i e^{i\mathbf{R}_i\mathbf{k}}s_{l,i}$) contains the energy of $|\Phi_0\rangle$ ($E_{\Phi_0}=\Sigma_q 2\varepsilon_{\mathbf{q}}$) plus four parts with the structures $e^{\dagger}h^{\dagger}s$, hes, $e^{\dagger}es$, and $h^{\dagger}hs$, respectively. The $e^{\dagger}h^{\dagger}s$ part, for example, is given by $(J/4N^{1/2})[(e^{\dagger}_{\mathbf{p}\uparrow}h^{\dagger}_{\mathbf{q}\downarrow}-e^{\dagger}_{\mathbf{p}\downarrow}h^{\dagger}_{\mathbf{q}\uparrow})s_{0,-\mathbf{q}-\mathbf{p}}+\sqrt{2}e^{\dagger}_{\mathbf{p}\uparrow}h^{\dagger}_{\mathbf{q}\uparrow}s_{-1,-\mathbf{q}-\mathbf{p}}+\sqrt{2}e^{\dagger}_{\mathbf{p}\downarrow}h^{\dagger}_{\mathbf{q}\downarrow}s_{1,-\mathbf{q}-\mathbf{p}}]$. This term of the Hamiltonian implies that $|\Phi_0\rangle$ is not the ground state (because it is not an eigenstate) of H when $J\neq 0$.

A. Unitary transformations

One of the most important steps in the analysis of this section is to determine a unitary transformation that modifies the ground state and the Kondo Hamiltonian and therefore maps the basic operators $c_{\mathbf{k}\alpha}$, $s_{l,\mathbf{k}}$ into a new set $\tilde{c}_{\mathbf{k}\alpha}=e^{-\tilde{T}}c_{\mathbf{k}\alpha}e^{\tilde{T}}$, $\tilde{s}_{l,\mathbf{k}}=e^{-\tilde{T}}s_{l,\mathbf{k}}e^{\tilde{T}}$ ($\tilde{T}^{\dagger}=-\tilde{T}$), such that $\tilde{e}_{\mathbf{p}\alpha}$ and $\tilde{h}_{\mathbf{q}\alpha}$ annihilate the *actual* interacting ground state $|\Phi\rangle$. We demand that $\tilde{T}$ should preserve the charge, lattice translational, and spin rotational symmetries of H since in the ground state $|\Phi\rangle$ no symmetry is broken. The simplest operator involving fermions that satisfies this condition is

$$\tilde{T}=\frac{J}{4N^{1/2}}\tilde{T}(\mathbf{k},\mathbf{k}')[(\tilde{c}^{\dagger}_{\mathbf{k}\uparrow}\tilde{c}_{\mathbf{k}'\uparrow}-\tilde{c}^{\dagger}_{\mathbf{k}\downarrow}\tilde{c}_{\mathbf{k}'\downarrow})\tilde{s}_{0,\mathbf{k}'-\mathbf{k}}+\sqrt{2}\tilde{c}^{\dagger}_{\mathbf{k}\uparrow}\tilde{c}_{\mathbf{k}'\downarrow}\tilde{s}_{-1,\mathbf{k}'-\mathbf{k}}+\sqrt{2}\tilde{c}^{\dagger}_{\mathbf{k}\downarrow}\tilde{c}_{\mathbf{k}'\uparrow}\tilde{s}_{1,\mathbf{k}'-\mathbf{k}}], \tag{13}$$

where $\tilde{T}^{*}(\mathbf{k}',\mathbf{k})=-\tilde{T}(\mathbf{k},\mathbf{k}')$ in order to satisfy $\tilde{T}^{\dagger}=-\tilde{T}$ and, as in all the equations throughout this section, repeated

indexes imply sum over them. This sum can be divided into four parts in terms of electrons and holes.

For small values of J, the new operators are expected to be slight deformations of the initial ones, and we can make the approximations

$$c^{\dagger}_{\mathbf{k}\alpha}=\tilde{c}^{\dagger}_{\mathbf{k}\alpha}+[\tilde{T},\tilde{c}^{\dagger}_{\mathbf{k}\alpha}],\quad s_{l,\mathbf{k}}=\tilde{s}_{l,\mathbf{k}}+[\tilde{T},\tilde{s}_{l,\mathbf{k}}]. \tag{14}$$

Substituting these expressions into the Hamiltonian, we obtain the expression of H in terms of the transformed operators $\tilde{e}_{\mathbf{p}\alpha}$, $\tilde{h}_{\mathbf{q}\alpha}$, and $\tilde{s}_{l,i}$.

Obviously, the terms of $\tilde{T}$ proportional to $\tilde{T}(\mathbf{p},\mathbf{p}')$ and $\tilde{T}(\mathbf{q},\mathbf{q}')$ do not contribute to changing the vacuum state in the leading order, therefore, we should consider that $\tilde{T}(\mathbf{p},\mathbf{p}')=\tilde{T}(\mathbf{q},\mathbf{q}')=0$. $\tilde{T}(\mathbf{p},\mathbf{q})$ and $\tilde{T}(\mathbf{q},\mathbf{p})$ are determined by requiring that the terms of the Hamiltonian of the form $\tilde{e}^{\dagger}\tilde{h}^{\dagger}\tilde{s}$ should be canceled in H, since their presence would imply that $|\Phi\rangle$ is not an eigenstate of H and, hence, not the ground state. This condition implies that $\tilde{T}(\mathbf{p},\mathbf{q})=-\tilde{T}(\mathbf{q},\mathbf{p})=1/(\varepsilon_{\mathbf{p}}-\varepsilon_{\mathbf{q}}+\tilde{\eta})$, where $\tilde{\eta}$ is given by $\tilde{\eta}=(3J^2/8)\ln 1/2\tilde{\eta}$. The introduction of the infrared regulator $\tilde{\eta}$ is necessary to achieve the cancellation of the $\tilde{e}^{\dagger}\tilde{h}^{\dagger}\tilde{s}$ terms of H in the low-energy region where higher-order terms give important contributions, and to ensure the unitarity of the transformation (14) to leading order in J.[28]

Using the above expression of $\tilde{T}(\mathbf{k},\mathbf{k}')$, we can readily calculate H in terms of $\tilde{e}_{\mathbf{p}\alpha}$, $\tilde{h}_{\mathbf{q}\alpha}$, and $\tilde{s}_{l,i}$. From the many terms that are generated in this change of coordinates, we select only those that are dominant for small J. A careful analysis shows that, in this regime, the Hamiltonian is essentially given by[28]

$$H=\tilde{C}+\tilde{H}_{\text{kinetic}}+\tilde{H}_{\text{Kondo}}+\tilde{H}_{\text{RKKY}}, \tag{15}$$

where

$$\tilde{C}=-\sum_{\mathbf{q}}2\tilde{E}(-\varepsilon_{\mathbf{q}})=E_{\Phi_0}-\frac{3J^2}{8}N\ln 2,$$

$$\tilde{H}_{\text{kinetic}}=\sum_{\mathbf{p},\alpha}\tilde{E}(\varepsilon_{\mathbf{p}})\tilde{e}^{\dagger}_{\mathbf{p}\alpha}\tilde{e}_{\mathbf{p}\alpha}+\sum_{\mathbf{q},\alpha}\tilde{E}(-\varepsilon_{\mathbf{q}})\tilde{h}^{\dagger}_{\mathbf{q}\alpha}\tilde{h}_{\mathbf{q}\alpha},$$

$$\tilde{E}(\varepsilon)=\varepsilon+\frac{3J^2}{16}\left[\left(1-\frac{3J^2}{16}\frac{1}{\varepsilon+\tilde{\eta}}\right)\ln\frac{\varepsilon+1/2}{\varepsilon+\tilde{\eta}}+\frac{\tilde{\eta}}{\varepsilon+\tilde{\eta}}\right]$$

$$(\varepsilon>0), \tag{16}$$

$$\begin{aligned}\tilde{H}_{\text{Kondo}}=&\frac{J}{4N^{1/2}}[(\tilde{e}^{\dagger}_{\mathbf{p}\uparrow}\tilde{e}_{\mathbf{p}'\uparrow}-\tilde{e}^{\dagger}_{\mathbf{p}\downarrow}\tilde{e}_{\mathbf{p}'\downarrow})\tilde{s}_{0,\mathbf{p}'-\mathbf{p}}\\&+\sqrt{2}\tilde{e}^{\dagger}_{\mathbf{p}\uparrow}\tilde{e}_{\mathbf{p}'\downarrow}\tilde{s}_{-1,\mathbf{p}'-\mathbf{p}}+\sqrt{2}\tilde{e}^{\dagger}_{\mathbf{p}\downarrow}\tilde{e}_{\mathbf{p}'\uparrow}\tilde{s}_{1,\mathbf{p}'-\mathbf{p}}]\\&+\frac{J}{4N^{1/2}}[(\tilde{h}^{\dagger}_{\mathbf{q}\uparrow}\tilde{h}_{\mathbf{q}'\uparrow}-\tilde{h}^{\dagger}_{\mathbf{q}\downarrow}\tilde{h}_{\mathbf{q}'\downarrow})\tilde{s}_{0,\mathbf{q}'-\mathbf{q}}\\&-\sqrt{2}\tilde{h}^{\dagger}_{\mathbf{q}\uparrow}\tilde{h}_{\mathbf{q}'\downarrow}\tilde{s}_{-1,\mathbf{q}'-\mathbf{q}}-\sqrt{2}\tilde{h}^{\dagger}_{\mathbf{q}\downarrow}\tilde{h}_{\mathbf{q}'\uparrow}\tilde{s}_{1,\mathbf{q}'-\mathbf{q}}],\end{aligned}$$

$$\tilde{H}_{\text{RKKY}}=\frac{1}{2}\sum_{i\neq j}J_{\text{RKKY}}(\mathbf{R}_i-\mathbf{R}_j)\tilde{\mathbf{S}}_i\cdot\tilde{\mathbf{S}}_j,$$

$$J_{\text{RKKY}}(\mathbf{R})=\frac{J^2}{V^2}\int d\mathbf{p}\,d\mathbf{q}\left(\frac{\varepsilon_{\mathbf{p}}}{\varepsilon_{\mathbf{p}}-\varepsilon_{\mathbf{q}}+\tilde{\eta}}-2\right)\frac{\cos[(\mathbf{q}-\mathbf{p})\cdot\mathbf{R}]}{\varepsilon_{\mathbf{p}}-\varepsilon_{\mathbf{q}}+\tilde{\eta}}. \tag{17}$$

V in this last equation stands for the volume of the first Brillouin zone.

B. Comments on the RKKY term

The RKKY interaction is directly drawn from the KLM. This is a success of our analysis since, to our knowledge, in the literature the RKKY interaction has always been added artificially to the Hamiltonian. Since all the terms in Eq. (15) containing fermionic operators with tildes annihilate $|\Phi\rangle$, the RKKY interaction is the only one responsible for the spin dynamics at $T=0$ provided that $|\Phi\rangle$ is stable with respect to the electronic part (we shall see that this is only the case for J smaller than a critical value). Thus, we can conclude that the magnetic nature of the ground state (quasiparticle spin-liquid, weak antiferromagnetism, magnetic fluctuations, etc.) must not be necessarily attributed to the competition between the Kondo interactions and the RKKY term.[29,30] We think that the magnetic behavior of this ground state arises from the very long-range character of the RKKY interaction (17), which leads to strong frustration and to spin fluctuations that tend to favor the formation of a quasiparticle spin liquid.[28]

Kagan and collaborators[3] are persuaded that the Kondo lattice can explain the HF state and that the huge specific heat at low temperature of this state may arise from the large increase of entropy associated with the thermal breakdown of the magnetic order induced by the RKKY interaction. We consider that this argument may be speculative but plausible. In any case, we are in agreement with these authors in that the renormalization effects on the charged spectrum by themselves can hardly account for the huge effective masses associated to the HF state and they cannot justify the existence of the enormous entropy at the Kondo lattice temperature (that is of the order $N\ln 2$).

The physical pattern of the system yielded by the KLM formalism is a vacuum state consisting of RKKY-induced spin correlations, and two kinds of elementary modes: soft neutral modes associated with deformations of the spin liquid, which lead to very large low-temperature values of the heat capacity and magnetic susceptibility, and charged modes corresponding to the excitation of electrons and holes in the system. A study of the spin correlations requires a quantum solution of the long-range-interaction Heisenberg

model (17) which is beyond the aim of this initial study. Nevertheless, we notice that while the Kondo term is proportional to J, the corresponding RKKY term varies proportionally to J^2. For instance, in one dimension, and considering an energy band dispersion as $\varepsilon_k = a|k|/\pi - 1/2$ where a is the real lattice constant, Eq. (17) takes the form

$$J_{\mathrm{RKKY}}(R) = J^2 \int_0^{1/2} dx \int_0^{1/2} dy \left(\frac{y}{1/2+y-x+\tilde{\eta}} - 2 \right) \times \frac{\cos[(1/2+y)\pi R/a]\cos(x\pi R/a)}{1/2+y-x+\eta}. \quad (18)$$

Carrying out this integral, we find that for the one-dimensional case, $J_{\mathrm{RKKY}}(R=na) = 0.26J^2$, $-0.20J^2$, $0.14J^2$, $-0.09J^2$, $0.07J^2, \ldots$, for $n = \pm 1, \pm 2, \pm 3, \pm 4, \pm 5, \ldots$, respectively, which corresponds to a weak antiferromagnetic term that can be neglected for small values of J as compared to the Kondo term. Thus, we will concentrate on the charged excitations, neglecting in its calculation the effect of the spin correlations. It should be pointed out here that, if the spin correlations were taken into account (considering always the *normal* state, where there is no magnetic order), we should also have to consider the terms in Eq. (15) containing two fermionic and two spin operators because, in this case, they give contributions to the dispersion relation of the charged modes that are of the same order as the spin correlations.

C. Ansatz formed by charged particles and neutral particles

In this subsection, we intend to give a solution of the Schrödinger equation whose Hamiltonian is given by Eqs. (15)–(17). This is performed via a variational procedure by means of a trial function. This function is constituted by an ansatz constructed by charged excitations coupled to spin fluctuation quasiparticles. Due to the electron-hole and spin rotational symmetries, we only need to consider, for instance, the negatively charged modes and the state in each spin multiplet with the highest s^z value. From Eq. (16) we see that the band structure of the states $\tilde{e}^{\dagger}_{\mathbf{p}\alpha}|\Phi\rangle$ and $\tilde{h}^{\dagger}_{\mathbf{q}\alpha}|\Phi\rangle$ contains a gap of magnitude $2\tilde{E}(0) = \tilde{\eta} + 3J^2/16$. These states, however, are *not* energy eigenstates. To find the true eigenstates, we build up the ansatz that is formed by modes that are small deformations of the states $\tilde{e}^{\dagger}_{\mathbf{p}\alpha}|\Phi\rangle$ for small values of J and with the condition $s = s^z = 1/2$ they can have the structure[28] $|UE_{\mathbf{p}\uparrow}\rangle = \alpha(\mathbf{p})[\tilde{e}^{\dagger}_{\mathbf{p}\uparrow} - (J/4N^{1/2})\beta_{\mathbf{p}}(\mathbf{p}')(\tilde{e}^{\dagger}_{\mathbf{p}'\uparrow}\tilde{s}_{0,\mathbf{p}-\mathbf{p}'} + \sqrt{2}\tilde{e}^{\dagger}_{\mathbf{p}'\downarrow}\tilde{s}_{1,\mathbf{p}-\mathbf{p}'})]|\Phi\rangle$, where $\alpha(\mathbf{p})$ is a normalization factor and $\beta_{\mathbf{p}}(\mathbf{p}')$ is a variational function that is determined as an extreme of the energy. This ansatz bears a strong parallel with that used to study the charged modes of the one-electron Kondo lattice[32] or the renormalization of the f states in the Anderson lattice model.[2] A simple calculation[28] shows that the energy decrease at the Fermi level of the slightly correlated modes (we call them uncorrelated modes) $|UE_{\mathbf{p}\alpha}\rangle$ with respect to $\tilde{e}^{\dagger}_{\mathbf{p}\ \mathrm{Fermi}\ \alpha}|\Phi\rangle$ closes the gap in the dispersion relation of $\tilde{H}_{\mathrm{kinetic}}$, as is physically expected.

It can be seen that, to suitably account for the high-energy tail of the Kondo coupling, these modes should be constructed from optimal operators $\hat{c}_{\mathbf{k}\alpha}, \hat{s}_{l,\mathbf{k}}$ such that the states $\hat{e}^{\dagger}_{\mathbf{p}\alpha}|\Phi\rangle$ are the best possible approximations for the actual uncorrelated electronic modes ($|UE_{\mathbf{p}\uparrow}\rangle$). These operators are obtained by means of a second transformation $\hat{T}$, which must have the general structure (13) in order to preserve all symmetries. In addition, this second transformation must leave $|\Phi\rangle$ invariant, and therefore, $\hat{T}(\mathbf{p},\mathbf{q}) = 0$. As we have commented regarding the states $|UE_{\mathbf{p}\uparrow}\rangle$, the effect of the Kondo interaction in the low-energy region of the electronic spectrum is to lower the energy. Therefore, in order to determine $\hat{T}(\mathbf{p},\mathbf{p}')$, we will demand that the energy of $\hat{e}_{\mathbf{p}_{\mathrm{Fermi}}\alpha}|\Phi\rangle$ be minimized. This leads to the result[28] $\hat{T}(\mathbf{p},\mathbf{p}') = (\varepsilon_{\mathbf{p}} - \varepsilon_{\mathbf{p}'})/[(\varepsilon_{\mathbf{p}} - \varepsilon_{\mathbf{p}'})^2 + \hat{\eta}^2]$, where $\hat{\eta}$ is given by $\hat{\eta} = (3\pi J^2/64)\ln 1/2\hat{\eta}$ [a completely analogous expression is obtained for $\hat{T}(\mathbf{q},\mathbf{q}')$].

Following the same steps as we did with the first transformation, we now find that the expression of H in terms of the operators with carets is essentially given by $H = \tilde{C} + \hat{H}_{\mathrm{kinetic}} + \hat{H}_{\mathrm{Kondo}} + \hat{H}_{\mathrm{RKKY}}$, where the Hamiltonians with carets have the same general structure as the corresponding ones with tildes [see Eqs. (17)] but with two important differences: first, the gap in the dispersion relation $\hat{E}(\varepsilon)$ is strongly reduced with respect to that in $\tilde{E}(\varepsilon)$, and has the estimated value $2\hat{E}(0)$ (Ref. 28) where $\hat{E}(0) = (3J^2/16)(\ln\pi/4 + 1/2) = 0.048J^2$, Second, instead of the coupling J, $\hat{H}_{\mathrm{Kondo}}$ contains a Kondo coupling[28] of the type $\hat{J}(\varepsilon_1,\varepsilon_2)$, which is effective only between electrons (or between holes) of very similar energies: $\hat{J}(\varepsilon_1,\varepsilon_2) = J\hat{\eta}^2/[(\varepsilon_1 - \varepsilon_2)^2 + \hat{\eta}^2]$. From the optimal operators $\hat{c}_{\mathbf{k}\alpha}, \hat{s}_{l,\mathbf{k}}$ we can now construct the SC modes. The general structure of an electron strongly correlated with a spin wave (such a state will be called henceforth SCE state), of $s = s^z = 1/2$ and wave vector $\mathbf{k}$, is given by

$$|\mathrm{SCE}_{\mathbf{k},1/2}\rangle = N^{-1/2}AB(\mathbf{p})(\hat{e}^{\dagger}_{\mathbf{p}\uparrow}\hat{s}_{0,\mathbf{k}-\mathbf{p}} + \sqrt{2}\hat{e}^{\dagger}_{\mathbf{p}\downarrow}\hat{s}_{1,\mathbf{k}-\mathbf{p}})|\Phi\rangle, \quad (19)$$

where A is a normalization factor and $B(\mathbf{p})$ a variational function that should minimize the energy (measured with respect to the energy of $|\Phi\rangle$):

$$E_{\mathrm{SC},1/2}[B] = A^2\left[\frac{3}{V}\int d\mathbf{p}\hat{E}(\varepsilon_{\mathbf{p}})B^*(\mathbf{p})B(\mathbf{p}) - \frac{3}{2V^2}\int d\mathbf{p}d\mathbf{p}'B^*(\mathbf{p}')\hat{J}(\varepsilon_{\mathbf{p}'},\varepsilon_{\mathbf{p}})B(\mathbf{p})\right].$$

We find[28] that the condition for the minimization of $E_{\mathrm{SC},1/2}$ has a solution *only* for antiferromagnetic couplings ($J > 0$). This solution (with the approximation $\hat{E}(\varepsilon) \sim \pm[\hat{E}(0) + \varepsilon]$, the sign + (−) is for particles (holes)) leads to $B(\mathbf{p}) = Z/[\varepsilon_{\mathbf{p}} + \Omega_{1/2}]$ and $E_{\mathrm{SC},1/2} = \pm[\hat{E}(0) - \Omega_{1/2}]$, where Z is an arbitrary constant that is determined by the normalization of the wave function $|\mathrm{SCE}_{\mathbf{k},1/2}\rangle$ and $\Omega_{1/2} = e^{-2/JD_F}/2$ and obviously the sign + (−) indicates that the wave functions are constructed with particle (hole) operators. For ferromag-

netic couplings, the local moments and the spin of the conduction electrons will tend to align parallel to each other and, if a collective state is formed, it should have the structure $|\mathrm{SCE}_{\mathbf{k},3/2}\rangle = N^{-1/2} CD(\mathbf{p}) \hat{e}^{\dagger}_{\mathbf{p}\uparrow} \hat{s}_{1,\mathbf{k}-\mathbf{p}} |\Phi\rangle$, which is the general form of a state composed of an electron and a spin wave having wave vector $\mathbf{k}$ and $s = s^z = 3/2$. In this case, the condition for minimizing $E_{\mathrm{SC},3/2}[D]$ has a solution only for $J<0$ and it leads to $D(\mathbf{p}) = Z/[\varepsilon_{\mathbf{p}} + \Omega_{3/2}]$, $E_{\mathrm{SC},3/2} = \pm[\hat{E}(0) - \Omega_{3/2}]$, where $\Omega_{3/2} = \mathrm{e}^{4/JD_F}/2$.

The energies $E_{\mathrm{SC},1/2}$ and $E_{\mathrm{SC},3/2}$ constitute the most important quantitative result of this section, since we have found the strongly correlated modes constructed from the coupling of the charged particles with spin fluctuations originated in the spin field. The flat bands of these strongly correlated modes will always be located at both sides of E_F, symmetrically distributed if the half-filling condition is used in the KLM analysis. In addition, we find that in ferromagnetic and antiferromagnetic Kondo lattices there is a tendency to form collective states of spin 3/2 and 1/2, respectively, and that, for couplings with the same strength, the formation of these states is much more favored in the antiferromagnetic case ($\Omega_{1/2} \gg \Omega_{3/2}$). If Ω stands for either $\Omega_{1/2}$ or $\Omega_{3/2}$, from the expressions of $B(\mathbf{p})$ and $D(\mathbf{p})$ it can be readily seen that the probability of finding in a SC mode an electron with wave vector $\mathbf{p}$ such that $\varepsilon \leqslant \varepsilon_{\mathbf{p}} \leqslant \varepsilon + d\varepsilon$ is $P(\varepsilon)d\varepsilon$, where $P(\varepsilon) \simeq \Omega/(\varepsilon + \Omega)^2$. This means, for instance, that 66% of the electrons in these modes have their wave vectors in the layer $0 \leqslant \varepsilon_{\mathbf{p}} \leqslant 2\Omega$. If $\Omega \ll \hat{E}(0)$, the energies of the SCE states are larger than those of the charged particles, and thus, they do not participate in the formation of SCE modes at low temperatures. On the contrary, these charged particles contribute at low temperatures to the SCE states if, with $\Omega < \hat{E}(0)$, both parameters are of the same order. In the latter case, the result will be a strong renormalization of the electron (and hole) masses around the Fermi level, since the band dispersion of the SCE mode is very flat. This would actually explain an important enhancement at the Fermi surface of the masses of the *charged* excitations measured by photoemission and dHvA experiments.[3] However, this electronic mass renormalization is not the main source of the heavy masses appearing in the HF state because the fraction of the band of charged particles that can participate in the formation of the SCE modes is small.[31] In any case, the presence of the SCE modes does not explain the enormous low-temperature entropy measured in these systems.[3]

IV. SUPERPOSITION OF THE RESULTS DRAWN FROM THE TWO ANALYSES

On the one hand, we have accounted for the charge fluctuation effects via the Hubbard Hamiltonian and the RPA to the self-energy. Our results show that the RPA linear response leads to a screened electron-electron Hubbard-like interaction whose corresponding GW self-energy produces low-energy quasiparticle structures that can be interpreted as transferences of spectral weight between the lower and upper Hubbard bands (this fact has been suggested in previous papers[12,20] corresponding to different strongly correlated systems). These features (that we call MHB) are not narrow enough to justify the large electron masses, but they are basically in agreement (aside from the peaks located just above and below E_F) with photoemission and dHvA data, and are essentially temperature independent.

The second and complementary analysis excludes the f-electron hopping between the f-electron atoms, since we consider that the spin field is always $s = 1/2$. It imposes the prohibition of f-band formation and in addition the f charge particle spectra are not considered (therefore, the MHB should be absent in this calculation). In addition to the renormalized Fermi liquid of extended states, the Kondo model yields two very flat bands that arise from the coupling between charged conduction particles and spin fluctuations waves, which generates the Kondo peaks. These peaks are symmetrically located below and/or above a small gap that contains the Fermi level. The number of nonlocalized electrons of the conduction band of the Kondo Hamiltonian that participate in the formation of the band of states $|\mathrm{SCE}_{\mathbf{k}}\rangle$ is small, because only in a narrow energy interval are there conduction electrons whose corresponding $B(\mathbf{p})$ functions have appreciable values. Therefore these two flat bands imply a not too much larger increase of the DOS just above and below E_F. By comparing our theoretical MHB of Sec. II to the experimental photoemission results,[5,6,11] we find discrepancies in the peaks just above and below E_F. It must be remembered that in our first calculation we only obtain a shoulder above E_F and the peak just below E_F is shorter than that located at -110 eV, while it is similar or even larger in the experimental results. The experimental fact that $\mathrm{CeSi}_{1.6}$ presents a softened peak above E_F with respect to CeSi_2 suggests that this peak is also due to extended p states, giving support to the conclusion that the structure just above E_F can also correspond (although not exclusively) to the Kondo peak obtained by the KLM analysis. The conduction electrons located in these flat bands of SCE states contribute to the electron masses, but as we have said above, the number of conduction electrons located in this band is small and, therefore, their contribution to the specific heat can be appreciable but not enough to justify the HF state. On the other hand, the HF state is characterized by the simultaneous appearance of a strong increase of entropy with an extremely large specific heat.[1,3] In Sec. III, we have explained that the spin correlations are the reason for a weak antiferromagnetic order whose exchange parameter varies as J^2, J being the Kondo parameter. This order can be broken at low temperatures and the magnetic breakdown can lead to a large increase of entropy (of about $N \ln 2$). As a consequence, an apparent effective large mass is detected in the specific heat measured in the HF state. Therefore, when considering each model separately, there are more discrepancies than agreements with the experimental results, but if one superposes the results drawn from the two models, namely, the middle-energy resonance, the flat bands of strongly correlated spin modes coupled with some (not many) conduction electrons, and the RKKY Hamiltonian, one may explain and reconcile the controverted spectroscopical results, the dHvA oscillations of the susceptibility, and the thermodynamic masses.

It is important to consider that two clearly distinct temperatures result from our analysis: the Kondo and the HF-state temperatures. In our second calculation, the Kondo temperature is given by the location with respect to E_F of the strongly correlated charged modes SCE, while the heavy-

fermion-state temperature is defined by the energy $K_B T_{\rm HF}$ necessary for the breakdown of the RKKY-induced magnetic correlations. Since the Kondo peaks correspond to the formation of collective states, it is clear that they will depend very strongly on temperature although, as we already mentioned, in a very different way than the Kondo resonances of the IAM do. On the contrary, the MHB spectrum is almost invariable with the temperature since it only varies via the Fermi function. Therefore, according to the results presented in this paper and concerning the controversy about the low-energy spectrum of the Ce systems in the HF state, we agree with Joyce and co-workers[5,7] in that the IAM cannot explain the low-energy features since the predicted spectrum is narrower than the PES data and wider than that necessary for justifying the specific heat, but we disagree with them when they conclude that the Kondo effect does not play any role in these systems. On the other hand our results support the results of Malterre *et al.*[6,10,11] in giving to the Kondo effect a preeminent role in the low-energy phenomena of these Ce compounds (in our analysis the Kondo lattice effects yields the SCE band states and the RKKY interaction producing antiferromagnetic correlations), but we disagree with their explanation of the photoemission spectra and the thermodynamical masses within the single IAM. Therefore, we believe that our results and our interpretation are equidistant from the interpretations of both experimental groups.

V. CONCLUSIONS

We have presented two complementary analyses of a Ce-based heavy-fermion compound that may reconcile the apparent contradictions between the photoemission and thermodynamic experiments. The spectrum results of the RPA calculation of Fig. 1 within the multiband Hubbard Hamiltonian represent an improvement with respect to those obtained within the impurity Anderson model[19] (see the comparision shown in Ref. 5). However, the main goal of our paper is not to show the improvements of the RPA results with respect to previous papers, but to try to reconcile the severe contradiction between the thermodynamical masses of the low-energy spectrum and those obtained with the spectroscopical and the dHvA experiments.[3] This is why we have performed, along with the RPA self-energy realistic calculation, an analysis in which only the Kondo lattice spin exchange that was excluded in this first calculation is considered. The fusion of the two analyses has four virtues:

(i) It proves that a screened interaction produced by charge fluctuations can basically reproduce the spectroscopical results of both the high- and low-energy quasiparticle structure, with the exception of the narrow Kondo-effect peaks, which obviously should be associated with the spin exchange. The bandlike nature of the low-energy spectrum[7,8] is in agreement with the results of our first calculation.

(ii) The effective masses and the topology of the Fermi surface detected by the dHvA experiments are in a fairly good agreement with the results obtained by the first calculation. Nevertheless, some quantitative discrepancies could be overcome by considering other self-energy approximations beyond the RPA, which somehow represents the simplest approach that can yield the three basic structures present in Ce systems.

(iii) The inclusion of the Kondo lattice analysis leads to a better description of the low-energy resonances, since the collective states that arise from the strong correlation between soft conductions electrons and spin fluctuations provide two symmetric peaks that must be added to the pattern obtained by the RPA calculation. The superposition of the two models yield a better agreement with the measured low-energy optical spectrum. It should be emphasized that these peaks have a completely different nature [see Eq. (19)] from those appearing in the IAM. Therefore, the temperature evolution of these structures, as well as the correlation between their widths and location and intensity, will be essentially different from that associated with the impurity Kondo resonances.

(iv) On the other hand, the second analysis brings into play the magnetic correlations induced by the RKKY interaction, which can give coherence between the relatively small spectroscopic and dHvA effective masses, and the very large masses arising from specific heat and magnetic susceptibility measurements.

ACKNOWLEDGMENTS

This work has been financed by the DGICYT (PB93-1249) and by the CIRIT (1995SGR 00039).

[1] Z. Fisk *et al.*, Science **239**, 33 (1988).
[2] K. Tsutsui *et al.* Phys. Rev. Lett. **76**, 279 (1996).
[3] Y. Kagan, K. A. Kikoin, and N. V. Prokof'ev, Physica B **182**, 201 (1992); **194**, 1171 (1994).
[4] F. López-Aguilar, J. Costa-Quintana, and L. Puig-Puig, Phys. Rev. B **48**, 1128 (1993); **48**, 1139 (1993); M. M. Sánchez-López *et al.*, Europhys. Lett. **27**, 235 (1994); J. Costa-Quintana *et al.*, Physica B **206&207**, 186 (1995).
[5] J. J. Joyce *et al.*, Phys. Rev. Lett. **68**, 236 (1992); F. J. J. Joyce and A. J. Arko, *ibid.* **70**, 1182 (1993); J. J. Joyce *et al.*, Physica B **186-188**, 31 (1993); **205**, 365 (1995); A. B. Andrews *et al.*, *ibid.* **206-207**, 83 (1995).
[6] F. Patthey *et al.*, Phys. Rev. Lett. **58**, 2810 (1987); **70**, 1179 (1993); D. Malterre *et al.*, Europhys. Lett. **20**, 445 (1992).
[7] A. B. Andrews, J. J. Joyce, A. J. Arko, J. D. Thompsom, J. Tang, J. M. Lawrence, and J. C. Hemminger, Phys. Rev. B **51**, 3277 (1995).
[8] A. B. Andrews, J. J. Joyce, A. J. Arko, Z. Fisk, and P. S. Riseborough, Phys. Rev. B **53**, 3317 (1996).
[9] A. J. Arko, J. J. Joyce, A. B. Andrews, J. L. Smith, J. D. Thompson, E. Moshopoulou, Z. Fisk, A. A. Menovsky, and P. C. Canfield, Physica B (to be published).
[10] D. Malterre *et al.*, Phys. Rev. Lett. **73**, 2005 (1994); **68**, 2656 (1992); E. Weschke *et al.*, *ibid.* **69**, 1792 (1992).
[11] D. Malterre *et al.*, Phys. Rev. B **48**, 10 599 (1993); M. Grioni *et al.*, *ibid.* **55**, 2056 (1997).
[12] P. Coleman, Physica B **206-207**, 872 (1995).
[13] M. M. Steiner *et al.*, Phys. Rev. B **43**, 1637 (1991).

[14] P. W. Anderson, Science **235**, 1196 (1987); Int. J. Mod. Phys. B **4**, 181 (1990); P. Coleman, Phys. World **8**, 29 (1995).
[15] F. Aryasetiawan and O. Gunnarsson, Phys. Rev. Lett. **74**, 3221 (1995).
[16] A. P. Kampf and J. R. Schrieffer, Phys. Rev. B **41**, 6399 (1990); **42**, 7967 (1990).
[17] T. C. Hsu and B. Douçot, Phys. Rev. B **48**, 2131 (1993); C. Chen, Phys. Rev. Lett. ; **73**, 1982 (1994); P. Unger, J. Igarashi, and P. Fulde, Phys. Rev. B **50**, 10 485 (1994); J. Igarashi, P. Unger, K. Hirai, and P. Fulde, *ibid.* **49**, 16 181 (1994); C. Calandra and F. Manghi, *ibid.* **50**, 2061 (1994); F. Manghi, C. Calandra, and O. Ossini, Phys. Rev. Lett. **73**, 3129 (1994); P. Unger and P. Fulde, Phys. Rev. B **51**, 9245 (1995).
[18] J. Costa-Quintana, M. M. Sánchez-López, and F. López-Aguilar, Phys. Rev. B **54**, 10 265 (1996).
[19] O. Gunnarsson and K. Schönhammer, in *Handbook of Physics and Chemistry of Rare Earths*, edited by K.A Gschneidner, Jr., L.J. Eyring, and S. Hufner (Elsevier, Amsterdam, 1987), Vol 10.
[20] N. Nücker *et al.*, Phys. Rev. B **51**, 8529 (1995); A. Krol *et al.*, *ibid.* **45**, 2581 (1992).
[21] M. M. Steiner, M. Alouani, R. C. Albers, and L. J. Sham, Physica B **199&200**, 186 (1994); M. M. Steiner, R. C. Albers, and L. J. Sham, Phys. Rev. Lett. **72**, 2923 (1994).
[22] P. A. Lee *et al.*, Comments Condens. Matter Phys. **12**, 99 (1986).
[23] P. Fulde, *Electron Correlations in Molecules and Solids* (Springer, Berlin, 1995), Chap. 12.
[24] K. Andres, J. E. Graebner, and H. R. Ott, Phys. Rev. Lett. **35**, 1779 (1975).
[25] G. R. Stewart, Rev. Mod. Phys. **56**, 755 (1984).
[26] T. M. Rice and K. Ueda, Phys. Rev. Lett. **55**, 995 (1985); Phys. Rev. B **34**, 6420 (1986).
[27] A. Millis and P. Lee, Phys. Rev. B **35**, 3394 (1986).
[28] J. M. Prats and F. López-Aguilar, Nucl. Phys. **B483**, 637 (1997).
[29] S. Doniach, Physica B **91**, 231 (1977).
[30] P. Coleman and N. Andrei, J. Phys., Condens. Matter. **1**, 4057 (1989).
[31] P. Nozières, Ann. Phys. (Paris) **10**, 19 (1985).
[32] M. Sigrist, H. Tsunetsugu, and K. Ueda, Phys. Rev. Lett. **67**, 2211 (1991).